

# Formation kinetics of magnetic chains, rings, X's, and Y's

Peter D. Duncan and Philip J. Camp\*

*School of Chemistry, University of Edinburgh, West Mains Road, Edinburgh EH9 3JJ, United Kingdom*

(Dated: May 5, 2017)

The kinetics of aggregation in a monolayer of magnetic particles are studied using stochastic dynamics computer simulations. At low densities ( $\leq 8\%$  coverage) the equilibrium structure is made up of chains and rings; the primary mechanisms by which these motifs form are described. At higher densities ( $> 15\%$  coverage), we observe large transient concentrations of Y-shaped and X-shaped defects that ultimately give way to an extended, labyrinthine network. Our results suggest that a defect mechanism – such as that proposed by Tlustý and Safran, *Science* **290**, 1328 (2000) – could drive a metastable phase separation in two dimensions.

PACS numbers: 75.50.Mm, 82.20.Wt, 82.70.Dd

The structure, phase behavior, and dynamics of strongly interacting, dipolar fluids present considerable challenges to soft-matter physics. The most common realization of a dipolar fluid is a ferromagnetic colloidal suspension, or ferrofluid. In the ideal case, this consists of spherical, homogeneously magnetized monodisperse particles with diameters  $\sim 10$  nm, sterically stabilized and immersed in a nonpolar solvent. The resulting colloidal interactions are caricatured by the widely studied dipolar hard sphere fluid. Despite almost four decades of intensive experimental, theoretical, and simulation study [1, 2], at least one outstanding question remains to be answered definitively: are point dipolar interactions alone sufficient to drive vapor-liquid phase separation?

On the one hand, the Boltzmann-weighted, angle average of the dipole-dipole potential gives (to leading order) an isotropic, attractive pair potential that varies like  $-1/r^6$ , where  $r$  is the interparticle separation; this is expected to produce conventional condensation behavior [3]. On the other hand, simulations show that conventional condensation is preempted by strong aggregation, driven at low temperatures by the energetically favorable ‘nose-to-tail’ conformation [4]. If phase separation occurs in 3D, then it is of a rather unusual nature; simulations suggest that the low-density phase mainly consists of chain-like aggregates, while the high-density phase resembles a network of interconnected segments [5]. One possible scenario involves a defect-mediated phase transition [6] in which the chains’ defects are the singly-connected particles at the chain ends, while the network’s defects consist of particles with three or four near neighbors in a Y-shaped or X-shaped conformation, respectively. Such fundamental issues are not only of relevance to magnetic fluids; the physical properties of many materials are governed by connectivity and topology [7].

Recently, 2D dipolar fluids (with 3D magnetostatics) have received attention due to the possibility of directly imaging aggregation in thin films using cryogenic transmission electron microscopy [8, 9, 10]. The equilibrium structure [11, 12] and dynamics [13] of 2D dipolar fluids have been studied in detail using computer simula-

tions. At low density and low temperature, the dominant structural motifs are isolated chains and rings. The high-density structure consists of a labyrinthine network of long chains, with a small concentration of X-shaped and Y-shaped defects. There has never been any suggestion of a vapor-liquid phase transition in the 2D system, but a transition between isolated and system-spanning clusters at low-density has recently been characterized [14]. The relative ease with which complex self-assembled structural motifs can be visualized and analyzed in experiments and simulations means that 2D fluids are attractive and important objects of study. Given the significance of such systems, it is surprising that more isn’t known about the self-assembly process itself, starting from a ‘random’ arrangement of particles. In one of the few studies in this area, Wen *et al.* directly imaged the aggregation of nickel-plated glass microspheres [15]. They observed that rings can be formed by two short chains joining at both ends simultaneously. Branching at X and Y defects was not considered.

In this Letter, we present a detailed simulation study of the aggregation process in monolayers of strongly dipolar particles. Starting from equilibrated configurations of non-polar particles, we elucidate the mechanisms of cluster formation that occur when the dipoles are ‘switched on’. At low densities, rings are predominantly formed by single, isolated chains folding up (rather than by the association of two short chains). Interestingly, at high densities, the system shows a high transient concentration of defect particles. This is significant because it suggests that highly branched structures could be stabilized kinetically. It might therefore be possible to realize a metastable, defect-mediated phase separation in the laboratory. We also briefly consider the types of mechanisms by which the structure evolves at long times.

We model the system as a monolayer of monodisperse dipolar soft spheres. The interparticle potential is given by

$$u(r, \boldsymbol{\mu}_1, \boldsymbol{\mu}_2) = 4\epsilon \left(\frac{\sigma}{r}\right)^{12} + \frac{\boldsymbol{\mu}_1 \cdot \boldsymbol{\mu}_2}{r^3} - \frac{3(\boldsymbol{\mu}_1 \cdot \mathbf{r})(\boldsymbol{\mu}_2 \cdot \mathbf{r})}{r^5} \quad (1)$$

where  $\epsilon$  is an energy parameter,  $\sigma$  is the sphere diameter,

$\boldsymbol{\mu}_i$  is the dipole vector on particle  $i$ ,  $\mathbf{r}$  is the interparticle separation vector, and  $r = |\mathbf{r}|$ . Reduced units are defined as follows: temperature  $T^* = k_B T / \epsilon$ , where  $k_B$  is Boltzmann's constant; dipole moment  $\mu^* = \sqrt{\mu^2 / \epsilon \sigma^3}$ ; particle number density  $\rho^* = \rho \sigma^2$ , where  $\rho = N / L^2$  and  $L$  is the length of the square simulation cell; time  $t^* = t / \tau$  where  $\tau = \sqrt{m \sigma^2 / \epsilon}$  is the basic unit of time. Stochastic dynamics simulations were performed according to the integrated Langevin equations [16]

$$\mathbf{r}_i(t + \delta t) = \mathbf{r}_i(t) + \frac{D_0^t}{k_B T} \mathbf{F}_i \delta t + \delta \mathbf{W}_i^t \quad (2)$$

$$\hat{\boldsymbol{\mu}}_i(t + \delta t) = \hat{\boldsymbol{\mu}}_i(t) + \frac{D_0^r}{k_B T} \mathbf{T}_i \wedge \hat{\boldsymbol{\mu}}_i(t) \delta t + \delta \mathbf{W}_i^r \wedge \hat{\boldsymbol{\mu}}_i(t) \quad (3)$$

where  $\mathbf{F}_i$  ( $\mathbf{T}_i$ ) is the net force (torque) acting on dipole  $i$  at time  $t$ ,  $\hat{\boldsymbol{\mu}}_i = \boldsymbol{\mu}_i / \mu$  is a unit dipole orientation vector,  $\delta t$  is the integration time step, and  $D_0^t$  ( $D_0^r$ ) is the translational (rotational) diffusion constant at infinite dilution. The components of the 2D vector  $\delta \mathbf{W}_i^t$  and the 3D vector  $\delta \mathbf{W}_i^r$  were generated independently from Gaussian distributions subject to the conditions  $\langle \delta \mathbf{W}_i^t \rangle = 0$ ,  $\langle \delta \mathbf{W}_i^t \cdot \delta \mathbf{W}_j^t \rangle = 4 D_0^t \delta t \delta_{ij}$ ,  $\langle \delta \mathbf{W}_i^r \rangle = 0$ , and  $\langle \delta \mathbf{W}_i^r \cdot \delta \mathbf{W}_j^r \rangle = 6 D_0^r \delta t \delta_{ij}$ . In this scheme, the short-time inertial dynamics are suppressed: with high dipole moments these occur on timescales of order 1 (in reduced units) [13], while of primary interest here are conformational processes occurring on timescales orders of magnitude longer.

We present results for  $N = 1024$  particles at a range of densities, with a large dipole moment  $\mu^* = 2.75$ , and temperature  $T^* = 1$ . Characteristic diffusion constants were estimated from the (stick) Stokes-Einstein laws yielding  $D_0^t = k_B T / 3 \pi \eta \sigma \simeq 4 \times 10^{-11} \text{ m}^2 \text{ s}^{-1}$  and  $D_0^r = k_B T / \pi \eta \sigma \simeq 1 \times 10^6 \text{ s}^{-1}$  for spherical particles with  $\sigma = 10 \text{ nm}$ , in a solvent of viscosity  $\eta = 10^{-3} \text{ Pa s}$  at temperature  $T = 300 \text{ K}$ ; the dimensionless quantities  $D_0^t \tau / \sigma^2 = 0.004$  and  $D_0^r \tau = 0.01$  were obtained using the mass for 10 nm spheres with mass density  $\sim 8000 \text{ kg m}^{-3}$  (typical for iron or cobalt) and energy parameter  $\epsilon = k_B T$ . The integration time step was  $\delta t^* = 0.01$ . Self-assembly was initiated from configurations generated with  $\mu^* = 0$ . For each density studied, five independent runs with different initial configurations were conducted, and the results for each density were averaged. The configurational temperatures associated with the positions and orientations of the particles were measured independently [17]. In all cases the instantaneous configurational temperatures fluctuated about  $T^* = 1$ , with rms deviations of about 0.1, throughout the self-assembly process.

At equilibrium, the low-density structure mainly consists of small rings and chains [13]. In Figs. 1(a)-(d) we show how a ring is formed by a chain closing in on itself, at a density  $\rho^* = 0.05$ . Wen *et al.* suggest that

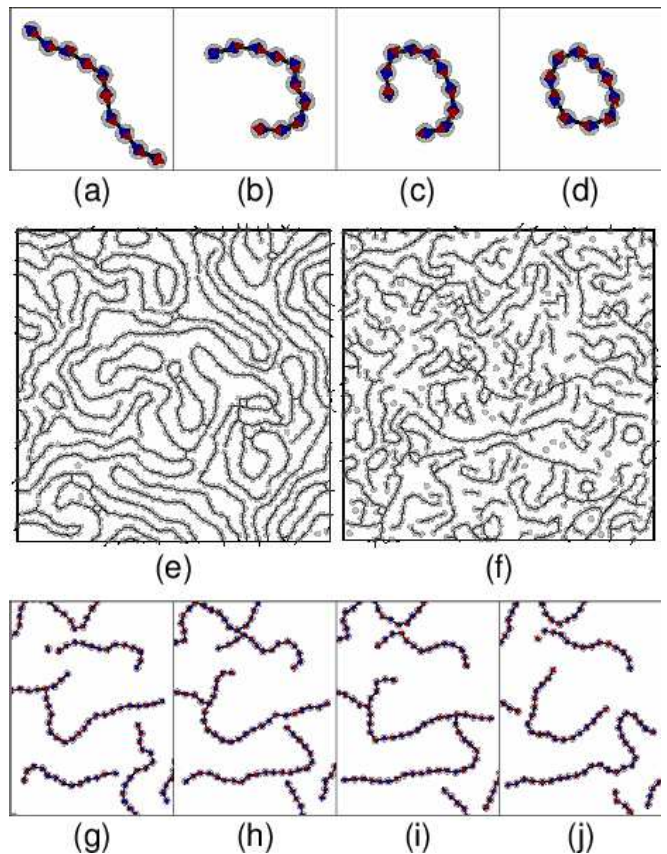


FIG. 1: (Color online) Instantaneous configurations at various densities and times: (a)  $\rho^* = 0.05$ ,  $t^* = 3500$ ; (b)  $\rho^* = 0.05$ ,  $t^* = 4330$ ; (c)  $\rho^* = 0.05$ ,  $t^* = 4800$ ; (d)  $\rho^* = 0.05$ ,  $t^* = 4950$ ; (e)  $\rho^* = 0.5$ ,  $t^* = 10000$ ; (f)  $\rho^* = 0.5$ ,  $t^* = 50$ ; (g)  $\rho^* = 0.2$ ,  $t^* = 1080$ ; (h)  $\rho^* = 0.2$ ,  $t^* = 1200$ ; (i)  $\rho^* = 0.2$ ,  $t^* = 1300$ ; (j)  $\rho^* = 0.2$ ,  $t^* = 1400$ . The black lines between particles denote ‘bonds’ identified using an energy criterion. In (a)-(d) and (g)-(j) the orientations of the dipole moments are indicated with red and blue cones.

rings are formed by two short chain-like segments making connections at either end simultaneously [15]. In contrast, movies of the aggregation process in our simulations show that the majority of rings are formed from isolated chains. At high density the equilibrium structure resembles a labyrinth of long, winding chains [13]; an ‘equilibrium’ configuration at  $\rho^* = 0.5$  is shown in Fig. 1(e). Locally, the equilibrium structures at low and high density are not so different; most particles are in chain-like environments, flanked by two near neighbors.

The process of self-assembly was monitored by identifying particles belonging to the same cluster on the basis of an energy criterion. We chose an energy cut-off of  $u_c = -0.6 \mu^{*2}$ , which captures a range of likely conformations for neighboring dipoles, either in chains or in more exotic defect environments [19]. We identified ‘terminal particles’ (one near neighbor), ‘internal particles’ (two near neighbors), ‘defect particles’ (three or more near neighbors), chains, rings, and ‘defect clusters’ (con-

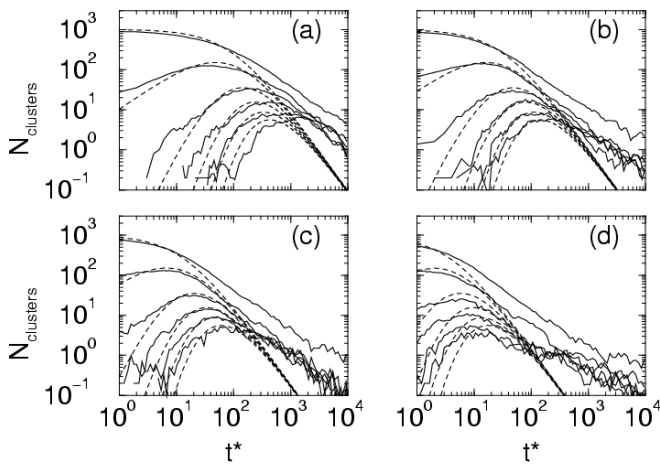


FIG. 2: Numbers of clusters containing (from top to bottom)  $n = 1, 2, 4, 6, 8,$  or  $10$  particles, as functions of time: (a)  $\rho^* = 0.1$ ; (b)  $\rho^* = 0.2$ ; (c)  $\rho^* = 0.3$ ; (d)  $\rho^* = 0.5$ . The solid lines are simulation results, and the dashed lines are fits to the von Smoluchowski model.

taining at least one defect particle).

In Fig. 2 we plot the numbers of  $n$ -mers ( $n = 1, 2, 4, 6, 8,$  and  $10$ ) as functions of time at densities in the range  $0.1 \leq \rho^* \leq 0.5$  [20]. To analyze the simulation results, we use a simple von Smoluchowski model [18]

$$\frac{d\rho_n}{dt} = \frac{1}{2} \sum_{i+j=n} k_{ij}\rho_i\rho_j - \rho_n \sum_{i=1}^{\infty} k_{ni}\rho_i \quad (4)$$

where  $\rho_n$  is the number density of  $n$ -mers, and the  $k_{ij}$ 's are 'rate constants'. Under the simplifying assumption that all rate constants are equal ( $k_{ij} = k$ ), the number of  $n$ -mers is  $N_n = N(k\rho t)^{n-1}/(1+k\rho t)^{n+1}$ , and the total number of clusters is  $\sum_{n=1}^{\infty} N_n = N/(1+k\rho t)$ , where  $\rho$  is the total number density of particles. We determined a reduced rate constant  $k^* = k\tau/\sigma^2$  for each density by fitting to the total number of clusters, with the results  $k^* = 0.049(3), 0.104(5), 0.156(4), 0.247(6),$  and  $0.52(1)$  at  $\rho^* = 0.05, 0.1, 0.2, 0.3,$  and  $0.5$ , respectively. The resulting curves for  $N_n(t)$  are shown in Fig. 2. The general level of agreement is quite good at short times, but at longer times the von Smoluchowski model underestimates the numbers of clusters. This is likely to be due to complex and slow relaxational processes occurring as the structure ripens, and the gross simplification of setting all rate constants equal.

In Fig. 3 we show the numbers of chains, rings, and defect clusters as functions of time at densities in the range  $0.1 \leq \rho^* \leq 0.5$ . At all densities, the numbers of chains are greater than the numbers of rings and defects during the early stages of the aggregation process, but the long-time behaviors are very different. Rings are favored over defect clusters at low density ( $\rho^* \leq 0.1$ ), in accord with the known equilibrium structures. At high density ( $\rho^* \geq 0.3$ ) defect clusters are favored over rings;

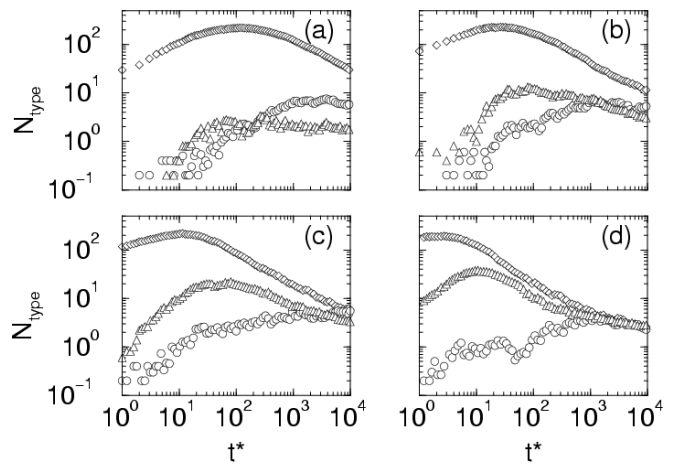


FIG. 3: Numbers of chains (excluding monomers) (diamonds), rings (circles) and defect clusters (triangles), as functions of time, at densities (a)  $\rho^* = 0.1$ , (b)  $\rho^* = 0.2$ , (c)  $\rho^* = 0.3$ , and (d)  $\rho^* = 0.5$ .

the numbers of defect clusters show strong maxima at intermediate times ( $t^* \sim 10-100$ ). At intermediate density ( $\rho^* = 0.2$ ) there are roughly equal numbers of rings and defect clusters.

To further elucidate the aggregation mechanisms, in Fig. 4 we plot  $x_n(t)$ , the fraction of particles with  $n$  neighbors ( $n = 0-4$ ) at time  $t$ , at densities in the range  $0.1 \leq \rho^* \leq 0.5$ . (No particles with five or more near neighbors were observed.) At all densities,  $x_0$  falls monotonically,  $x_1$  shows a maximum, and  $x_2 \rightarrow 1$  as the majority of particles ultimately end up with two neighbors as parts of chains or rings. Dramatic differences between low-density and high-density aggregation kinetics are evidenced by  $x_3$  and  $x_4$ . At low density ( $\rho^* \leq 0.1$ ) less than  $\sim 0.2\%$  of particles have three or more neighbors at any given time. At intermediate density ( $\rho^* = 0.2$ )  $x_3$  shows a maximum at  $t^* \sim 100$ , while  $x_4$  is essentially negligible. At higher densities ( $\rho^* = 0.3, 0.5$ ) and at intermediate times ( $t^* \sim 100$ ), up to  $10\%$  of all particles are defects, with approximately ten times more particles having three neighbors than four neighbors. In Fig. 1(f) we show a snapshot of a configuration at  $\rho^* = 0.5$  and  $t^* = 50$ , i.e., close to the location of the peak in  $x_3$ . Note the higher connectivities of particles within clusters as compared to those when the system is closer to equilibrium [ $t^* = 10000$ , Fig. 1(e)]. Ultimately, the number of defect particles falls again by at least an order of magnitude as equilibrium is approached.

Of course, aggregates continue to disassemble and form, even at equilibrium. During the aggregation process at high density, there is a very slow net decrease in the number of defect particles within the system. It is impossible to identify specific local events where the number of defects is reduced irreversibly, but in Figs. 1(g)-(j) we show a sequence of snapshots that illustrate the kinds

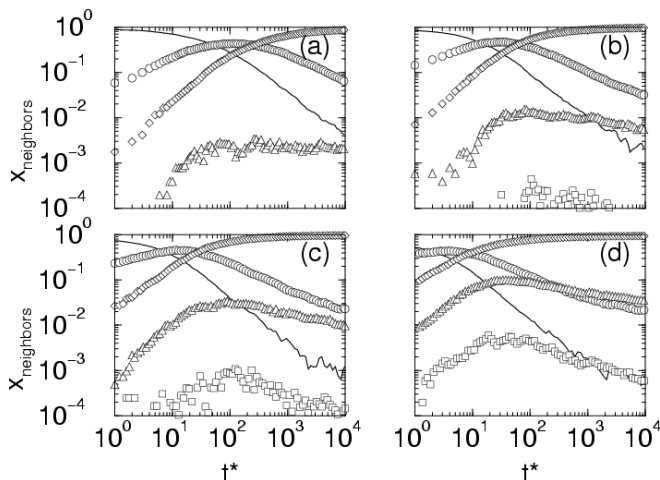


FIG. 4: Fractions of particles with  $n$  neighbors, as functions of time, at densities (a)  $\rho^* = 0.1$ , (b)  $\rho^* = 0.2$ , (c)  $\rho^* = 0.3$ , and (d)  $\rho^* = 0.5$ :  $n = 0$  (solid line);  $n = 1$  (circles);  $n = 2$  (diamonds);  $n = 3$  (triangles);  $n = 4$  (squares).

of processes which, in the long run, lead to a changing cluster distribution. The time interval  $t^* = 1080-1400$  corresponds to where  $x_3$  is decreasing relatively rapidly. In the upper regions of these figures, we see how two chains segments meet, bond temporarily, and then separate. In the lower halves of Figs. 1(g) and 1(h), we see how two chains can collide at right angles, and split in to two new chains. In Fig. 1(i), we see a cluster with two defect particles; in Fig. 1(j) we see the result of that cluster having ruptured at the positions of those two defects almost simultaneously.

In summary, our results show that the aggregation mechanisms at low density and high density are very different. At low density, aggregation proceeds through the formation of chains, some of which will go on to form rings, as shown in Fig. 1(a)-(d). At high density, it appears that the transient aggregates include a significant proportion of defect clusters, such as those implicated in 3D dipolar phase separation [6]. At equilibrium, the particle connectivities at low density and high density are somewhat similar in that the vast majority of particles have exactly two neighbors.

Our observations suggest a direct experimental test for the theory of defect-mediated phase transitions put forward by Tlusty and Safran [6]. If the ferrocolloid particles were modified to introduce a strong, short-range attraction (e.g. chemically, or with added polymer to induce depletion forces) then the transient network structure at high density may be kinetically stabilized long enough for phase separation to occur, even in thin films where no equilibrium transition is anticipated. This can only arise if the high-density branched structure corresponds to a

local free-energy minimum. The experimental approach suggested here could provide a way of guiding the dense phase in to that minimum, but there may be alternative strategies. In any case, we hope that aggregation kinetics and metastable phases in strongly dipolar fluids can be investigated by direct experimental observation.

We thank the School of Chemistry at the University of Edinburgh for the provision of an EPSRC DTA studentship to PDD.

\* Electronic address: philip.camp@ed.ac.uk

- [1] P. I. C. Teixeira, J. M. Tavares, and M. M. Telo da Gama, *J. Phys.: Condens. Matter* **12**, R411 (2000).
- [2] C. Holm and J.-J. Weis, *Curr. Opin. Colloid Interface Sci.* **10**, 133 (2005).
- [3] P. G. de Gennes and P. A. Pincus, *Phys. Kondens. Materie* **11**, 189 (1970).
- [4] J. J. Weis and D. Levesque, *Phys. Rev. Lett.* **71**, 2729 (1993).
- [5] P. J. Camp, J. C. Shelley, and G. N. Patey, *Phys. Rev. Lett.* **84**, 115 (2000).
- [6] T. Tlusty and S. A. Safran, *Science* **290**, 1328 (2000).
- [7] A. Zilman, T. Tlusty, and S. A. Safran, *J. Phys.: Condens. Matter* **15**, S57 (2003).
- [8] V. F. Puentes, K. M. Krishnan, and A. P. Alivisatos, *Science* **291**, 2115 (2001).
- [9] K. Butter, P. H. H. Bomans, P. M. Frederik, G. J. Vroege, and A. P. Philipse, *Nature Materials* **2**, 88 (2003).
- [10] M. Klokkenburg, R. P. A. Dullens, W. K. Kegel, B. H. Ern e, and A. P. Philipse, *Phys. Rev. Lett.* **96**, 037203 (2006).
- [11] J. M. Tavares, J. J. Weis, and M. M. Telo da Gama, *Phys. Rev. E* **65**, 061201 (2002).
- [12] J. J. Weis, *J. Phys.: Condens. Matter* **15**, S1471 (2003).
- [13] P. D. Duncan and P. J. Camp, *J. Chem. Phys.* **121**, 11322 (2004).
- [14] J. M. Tavares, J. J. Weis, and M. M. Telo da Gama, *arXiv:cond-mat/0505043*.
- [15] W. Wen, F. Kun, K. F. P al, D. W. Zheng, and K. N. Tu, *Phys. Rev. E* **59**, R4758 (1999).
- [16] R. B. Jones and F. N. Alavi, *Physica A* **187**, 436 (1992).
- [17] A. A. Chialvo, J. M. Simonson, P. T. Cummings, and P. G. Kusalik, *J. Chem. Phys.* **114**, 6514 (2001).
- [18] H. Sonntag and K. Strenge, *Coagulation kinetics and structure formation* (Plenum, New York, 1987).
- [19] Earlier work on the equilibrium clusters in dipolar hard sphere fluids employed a distance criterion [11]. The optimum cut-off depends sensitively on the short-range potential. Nonetheless, we have confirmed that a distance cut-off of  $1.5\sigma$  yields comparable results to those reported here.
- [20] We also studied  $\rho^* = 0.05$ , but the results are very similar to those at  $\rho^* = 0.1$  and are therefore omitted for brevity.